Sensors and Materials, Vol. 33, No. 11 (2021) 3693–3708
MYU Tokyo

S & M 2718

Application of Remote Sensing Technology to Monitoring of Vegetation Recovery and Regional Precipitation in Wenchuan Earthquake Area: Case Study of Longxi River Basin

Biyun Guo,[1,2*] Mantravadi Venkata Subrahmanyam,[1**]
Aiguo Li,[3] and Guangzhe Liu[4]

[1]Marine Science and Technology College, Zhejiang Ocean University, Zhoushan, Zhejiang 316022, China
[2]State Key Laboratory of Plateau Ecology and Agriculture, Qinghai University, Xining, Qinghai 810016, China
[3]Zhoushan Natural Resources Surveying and Mapping Design Centre, Zhoushan, Zhejiang 316022, China
[4]College of Forestry, Northwest A & F University, Yangling, Shaanxi 712100, China

(Received February 17, 2021; accepted May 11, 2021)

Keywords: precipitation, earthquake, normalized difference vegetation index (NDVI), vegetation coverage, remote sensing

The Wenchuan earthquake occurred in Sichuan Province, China, on May 12, 2008, and caused a large number of secondary geological disasters such as collapses, debris flows, and landslides, as well as extensive damage to local vegetation. The earthquake had an impact on the regional climate, seriously affecting the sustainable development of the regional environment and economy. In this study, the normalized difference vegetation index (NDVI) was used to characterize the vegetation status, which was calculated from images acquired by the MODIS sensor. Based on the vegetation cover and precipitation of the area affected by the Wenchuan earthquake over about 70 years, in this paper we analyze the characteristics of vegetation changes and their impact on the climate after the earthquake. The results revealed that the above secondary geological disasters caused by the earthquake destroyed vegetation. After the earthquake, NDVI decreased from 0.394 in 2007 to 0.383 on July 1, 2008, and then increased year by year to 0.413 in 2015, except in 2010. During the two years after the earthquake, several large-scale debris flows occurred in this area, damaging the surface vegetation, so the vegetation coverage was low in 2010. The change of the land cover has an indirect impact on the local precipitation. The annual and seasonal (except winter) precipitation trended downward from 1948 to 2018, with an annual average decrease of 1.6069 mm, but trended upward from 2008 to 2018, with an annual average increase of 14.012 mm, after the Wenchuan earthquake, indicating the recovery of vegetation. The increased vegetation promoted regional precipitation, but the interaction mechanism between the vegetation cover and the precipitation is complex. The effect of the vegetation differs in different regions and cannot be generalized. This study provides theoretical support for vegetation restoration and environmental management in areas with strong earthquakes.

*Corresponding author: e-mail: biyunguo@163.com
**Corresponding author: e-mail: mvsm.au@gmail.com
https://doi.org/10.18494/SAM.2021.3337

ISSN 0914-4935 © MYU K.K.
https://myukk.org/

1. Introduction

On May 12, 2008, an earthquake with the highest magnitude (8.0 on the Richter scale) and causing the most severe damage since the founding of the People's Republic of China occurred in Wenchuan County, Sichuan Province. The epicenter of the earthquake was 103.4° E, 31.0° N, the focal depth was 12–19 km, and the intensity was 11 degrees.(1) According to data from the Forestry Department of Sichuan Province, the loss of forested area was about 3.29×10^3 km^2, which resulted in a direct economic loss estimated to be as high as 35 million US dollars.(2) As well as causing casualties and property losses, the Wenchuan earthquake also caused a huge amount of damage to the ground surface. Secondary geological disasters, such as collapses, landslides, debris flows, and barrier lakes, caused serious damage to the terrestrial and river ecosystem, adversely affecting the environmental sustainability of the regional ecology and exacerbating regional climate change.(3–7)

The impact of ecosystem changes on the climate involves a complex process. Nobre *et al.* and Bagley *et al.*(8,9) studied the impact of deforestation on the climate by using a general circulation model. It was found that after replacing rainforest with grasslands, the surface temperature increased by 2.5 °C, the annual evapotranspiration rate decreased by 30%, precipitation decreased by 25%, and the dry season became more prevalent. Xue *et al.*(10) pointed out that as the Sahara Desert continues to expand, precipitation will decrease by 13% and evaporation and cloud cover will also decrease. When precipitation increases by 25%, evaporation also increases significantly, leading to de-desertification.(10) According to Wang,(11) when the grassland around Inner Mongolia is destroyed, the water cycle process in this area weakens, precipitation and evaporation decrease, the ground temperature increases, and the corresponding surface sensible heat flux and long-wave radiation flux increase. In contrast, the latent heat flux and absorbed solar short-wave radiation decrease, and the decreases in precipitation and evaporation are mainly related to the changes in the surface roughness and albedo of the sandy land.

Since the Wenchuan earthquake, the earthquake-stricken areas with damaged vegetation have been recovering. Several researchers have focused on geological disasters caused by earthquakes and the local changes in the environment, whereas there has been less research on changes in the climate during the post-earthquake restoration of vegetation.(12–18) Generally, vegetation restoration is a long-term biological process, which will inevitably affect the regional climate. Fu and Yuan(19) used a regional environmental system integration model (RIEMS)(20) to simulate the impact of natural vegetation restoration on the regional climate and environment in East Asia. The results indicated that the restoration of natural vegetation will strengthen the summer monsoon in East Asia. This will increase the transportation of water vapor to most of China, which will significantly increase the water vapor content in the atmosphere, increase precipitation and soil moisture, and thus markedly change the regional ecological environment. Spracklen and Garcia-Carreras estimated the impact of deforestation on precipitation in the Amazon Basin and found that in the case of business-as-usual deforestation (based on the deforestation before 2004), the average annual precipitation will be reduced by 8.1 ± 1.4% by 2050, which is greater than the natural change.(21)

Vegetation coverage in 2008 was reduced a result of the Wenchuan earthquake, and its sub-geological disasters such as landslides and mudslides damaged the vegetation, changing the soil water evapotranspiration and precipitation vegetation interception in the disaster area, which in turn affected the regional humidity, air pressure, temperature, and precipitation to different extents.(22,23) Vegetation plays an important role in global climate change and affects climate conditions. The normalized difference vegetation index (NDVI) can characterize the vegetation coverage and is related to plant transpiration, photosynthesis, and net primary productivity.

The process by which surface vegetation changes is an important factor affecting regional climate change. The spatial distribution of the vegetation type is the result of long-term climate adaptation and vegetation, which has a certain feedback effect on climate. Vegetation cover affects the radiation balance, water balance, and other processes by changing surface properties such as the surface albedo, roughness, and soil temperature, eventually leading to changes in regional precipitation, atmospheric circulation, and other phenomena. After the Wenchuan earthquake, the vegetation in the affected areas was damaged to various extents, which had an impact on local precipitation.(24–26) However, there are few studies on regional precipitation variations during the process of surface vegetation restoration after a strong earthquake. Therefore, it is necessary to analyze this issue in depth. Terra MODIS satellite sensor data products provide high-temporal-resolution vegetation coverage. This study focused on the relationship between vegetation and precipitation in an earthquake-stricken area. The analysis of the impact of vegetation on local precipitation after the earthquake will be helpful in providing a scientific basis for ecological restoration planning.

2. Study Area

The study site, Longxi River Basin (Fig. 1), is located in an area severely damaged by the Wenchuan earthquake. Belonging to the Longmen Mountain fault zone structurally and

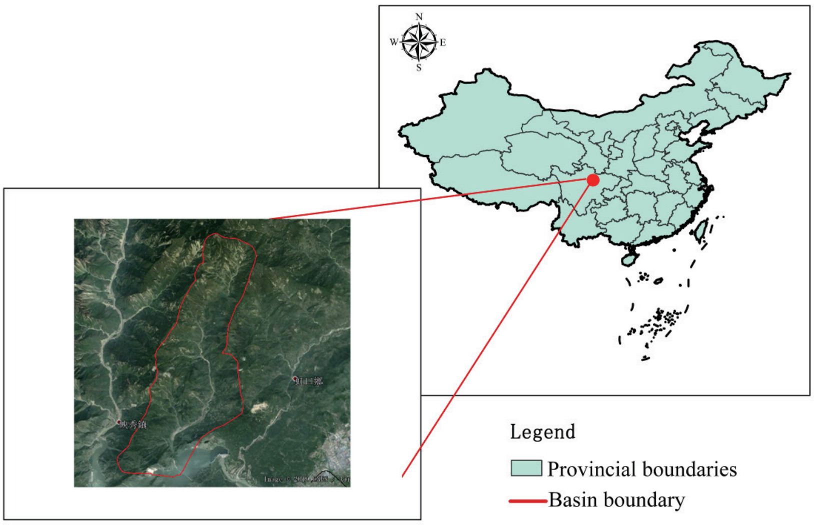

Fig. 1. (Color online) Location of Longxi River Basin.

traversing the study area, the Longxi River Basin is the main part of the Yingxiu–Beichuan fault zone causing the Wenchuan earthquake. Owing to severe rock fragmentation, the area is subjected to strong weathering and has become a typical area with tectonic instability.(27)

The 79 km^2 Longxi River Basin is part of the Minjiang River, which is a tributary of the upper Yangtze River watershed. The longitude and latitude ranges are 103.4992–103.6019° E and 31.0275–31.1789° N, respectively. The study area is located northwest of Du Jiang Yan City and has an altitude between 793 and 3290 m. Annual precipitation in the basin is 1134.8 mm, with 80% of the annual precipitation concentrated between May and September.(28) The regional geological structure is complex. The geology is mainly composed of volcanic rock, limestone, sandstone, and shale.(24) In part of the area near Du Jiang Yan City, an analysis of 53 years (from 1955 to 2008) of records revealed that the mean annual temperature is 15.2 °C.(28)

After the Wenchuan earthquake, geological disasters occurred progressively along the Longxi River Basin. On August 13, 2010, a debris flow (the "8.13 super-large debris flow") was triggered by heavy precipitation lasting for 90 min, which washed slope debris into the waterway and blocked a local river, raising the riverbed in the main channel by an average of 5–7 m.(25) The debris flow washed away a retaining wall, blocked a road, and then was swept into the lower Longxi River, where it was deposited as an aggregation with a length of 930 m, a width of 18 m, and a height of 6 m.(26) Figure 2 shows a house destroyed by the debris flow.

3. Materials and Methods

3.1 Precipitation

We analyzed the effect of the change in vegetation on precipitation using precipitation data over the study area from the Global Precipitation Climatology Project (GPCP) precipitation dataset. GPCP was established by the World Climate Research Program to develop a more complete understanding of the spatial and temporal patterns of global precipitation. GPCP provides global precipitation products with satellite and rain gauge information with 1° spatial resolution.(29) For this study, GPCP Version 1.3 data for the period from January 1, 1948 to December 31, 2018 was used.(30)

Fig. 2. (Color online) House destroyed by the debris flow along Longxi River Basin.

3.2 Remote sensing image

QuickBird satellite was launched in October 2001 by American Digital Globe Co. It is one of the commercial satellites providing images of earth with submeter resolution. The resolutions of QuickBird images are 0.61 m in the panchromatic band and 2.44 m in the multispectral band. Products include panchromatic, multispectral, panchromatic enhancement, and binding (panchromatic + multispectral) images (https://discover.digitalglobe.com/). In this study, two images taken before (June 26, 2005) and after (April 26, 2010) the earthquake, as shown in Fig. 3, were selected to analyze the geological disasters and vegetation changes. Figure 4 is a secondary geological hazard map obtained from the QuickBird image taken on April 26, 2010.

3.3 NDVI

Vegetation coverage is described by NDVI, which is an indicator of the plant growth status and the spatial distribution of vegetation. NDVI varies between −1.0 and +1.0, where a negative value indicates that the ground cover is cloud, water, snow, and so forth, which highly reflect visible light. A value of zero indicates rock or bare soil. A positive NDVI indicates vegetation coverage, and NDVI increases with the amount of coverage. Because vegetation grows luxuriantly in July, the NDVI of this month is selected to represent the local vegetation coverage and compare the vegetation in different years.

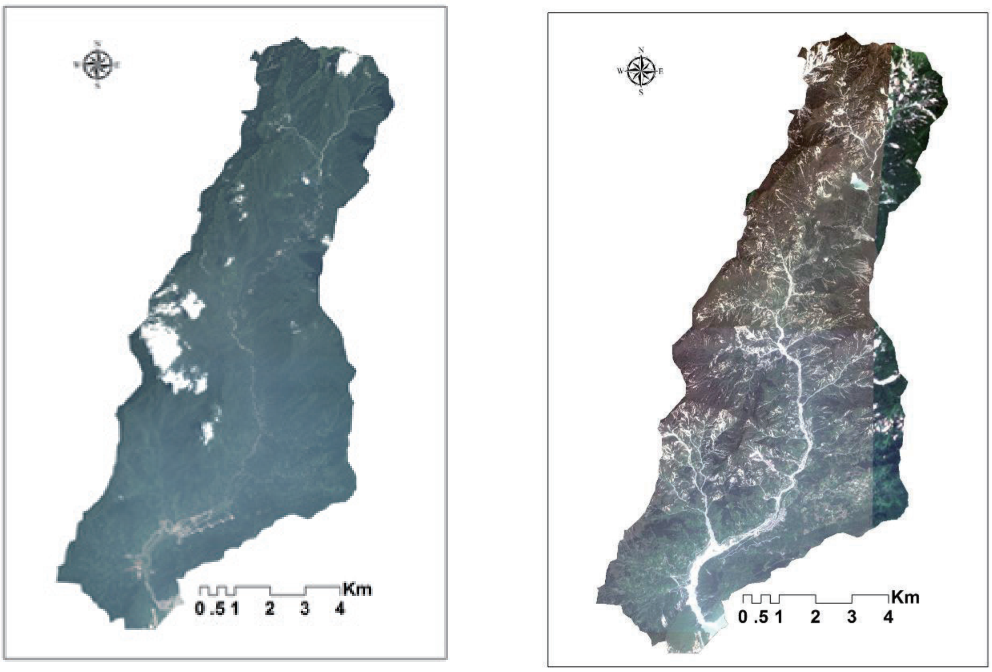

(a) (b)

Fig. 3. (Color online) QuickBird images of Longxi River Basin taken on (a) June 26, 2005 and (b) April 26, 2010.

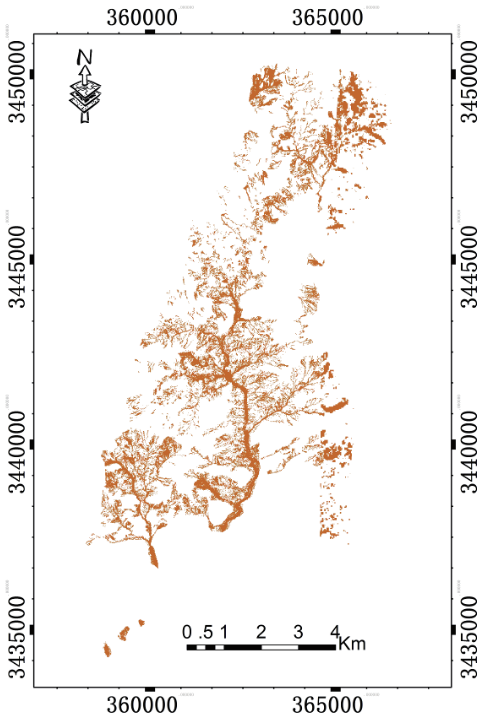

Fig. 4. (Color online) Secondary geological hazard map of Longxi River Basin after the earthquake.

NDVI is calculated from individual measurements as follows:

$$\mathrm{NDVI} = (\mathrm{NIR} - \mathrm{Red}) / (\mathrm{NIR} + \mathrm{Red}), \tag{1}$$

where Red and NIR respectively stand for the spectral reflectances measured in the red (visible, 0.58–0.68 μm) and near-infrared (0.725–1.1 μm) regions.

In this research, NDVI is calculated from MODIS images provided by the International Scientific & Technical Data Mirror Site, Computer Network Information Center, Chinese Academy of Sciences (http://www.gscloud.cn) using the following formula:

$$\mathrm{NDVI} = (B2 - B1) / (B2 + B1), \tag{2}$$

where B1 and B2 represent bands 1 and 2 of MODIS remote sensing images, respectively.

In this work, daily data of the NDVI from MODND1D over China with 500 m resolution and the monthly data of the Terra with 500 m resolution were processed by MOD09GA through projection conversion and other processes. The data is described in Table 1.

Table 1
NDVI of Longxi River Basin from 2001 to 2015.

Date	Data	Resolution
2001.7	MODND1M.20010701.CN.NDVI.MAX.V2	500 m
2004.7	MODND1M.20040701.CN.NDVI.MAX.V2	500 m
2007.7	MODND1M.20070701.CN.NDVI.MAX.V2	500 m
2008.7	MODND1M.20080701.CN.NDVI.MAX.V2	500 m
2010.7	MODND1M.20100701.CN.NDVI.MAX.V2	500 m
2012.7	MODND1M.20120701.CN.NDVI.MAX.V2	500 m
2014.7	MODND1M.20140701.CN.NDVI.MAX.V2	500 m
2015.7	MODND1M.20150701.CN.NDVI.MAX.V2	500 m

4. Results

4.1 Vegetation coverage

Figure 5 illustrates the changes in vegetation in the Longxi River Basin in July from 2001 to 2015. From the maps, the vegetation cover in the south is higher than that in the north, and the vegetation coverage decreased after the Wenchuan earthquake (2008) but increased in 2015. After the "5.12" Wenchuan earthquake, a large number of landslides occurred and debris accumulated at the slopes and gullies, which provided materials for the generation of debris flows. After the earthquake, several large debris flow disasters occurred in this area, such as the one on August 13, 2010, which further damaged the surface and reduced the vegetation coverage in the disaster area.

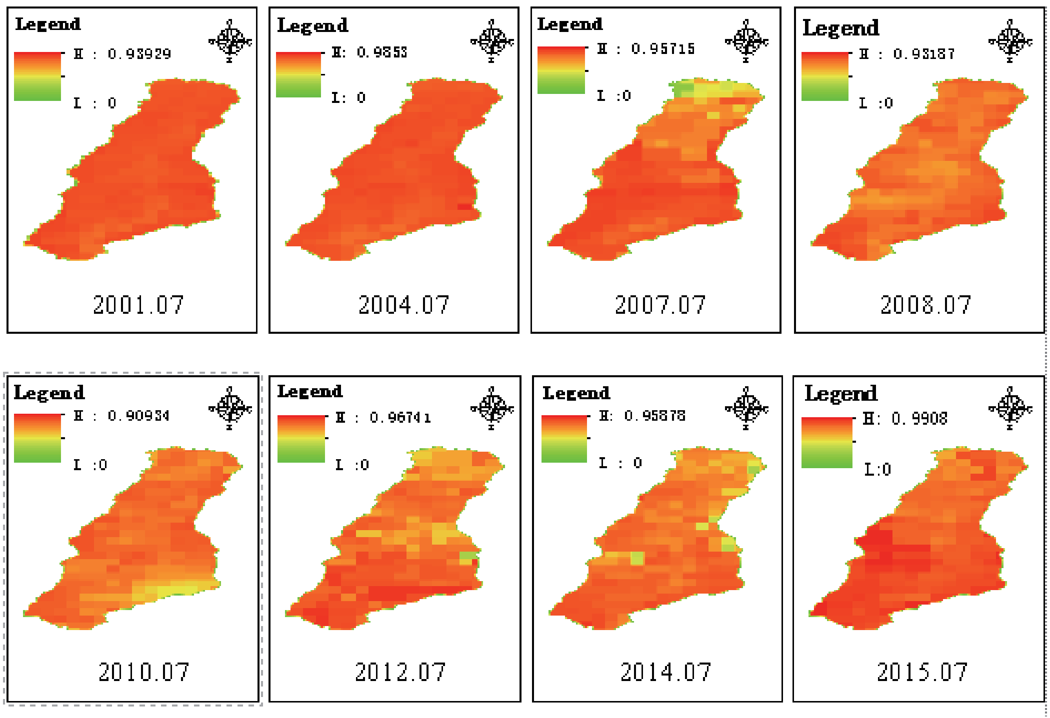

Fig. 5. (Color online) NDVI in Longxi River Basin from 2001 to 2015.

Table 2
NDVI values of Longxi River Basin in July from 2001 to 2015.

Value	2001	2004	2007	2008	2010	2012	2014	2015
Maximum	0.93929	0.9853	0.95715	0.93187	0.90934	0.96741	0.95878	0.9908
Minimum	0	0	0	0	0	0	0	0
Mean	0.417	0.418	0.394	0.383	0.373	0.382	0.373	0.413

The maximum and minimum values of NDVI reflect individual phenomena, and the mean value can represent the local general vegetation growth. The mean value was selected for this study. The statistical analysis of NDVI in different periods is presented in Table 2. The mean value of NDVI decreased in July after the Wenchuan earthquake (2008) and increased in 2015. The precipitation in spring 2007 was the second lowest (57.98 mm) in the time period examined and was only higher than the minimum value of 55.42 mm in spring 2000. This low precipitation affected the vegetation growth, and NDVI in 2007 was lower than that in previous years. After the earthquake, the vegetation coverage increased rapidly through artificial afforestation and ecological restoration.

4.2 Interannual variation of precipitation

Figures 6 and 7 respectively show the changes in annual precipitation in the Longxi River Basin from 1948 to 2018 and after the earthquake (from 2008 to 2018). It can be seen from Fig. 6 that the annual precipitation varies greatly, and the overall trend from 1948 to 2018 is a decline in precipitation. After the earthquake, the surface cover was seriously damaged and the fluctuation in annual precipitation was increased by the recovery of vegetation in the basin (Fig. 7).

The regression analysis of annual precipitation was carried out to obtain the trend equation from 1948 to 2018 and after the earthquake (2008 to 2018) and R^2. The equations and values of R^2 are as follows:

$$y = -1.6069x + 4161,\ R^2 = 0.0586 \text{ (1948 to 2018)}, \quad (3)$$

$$y = 14.012x - 27211,\ R^2 = 0.2715 \text{ (2008 to 2018)}. \quad (4)$$

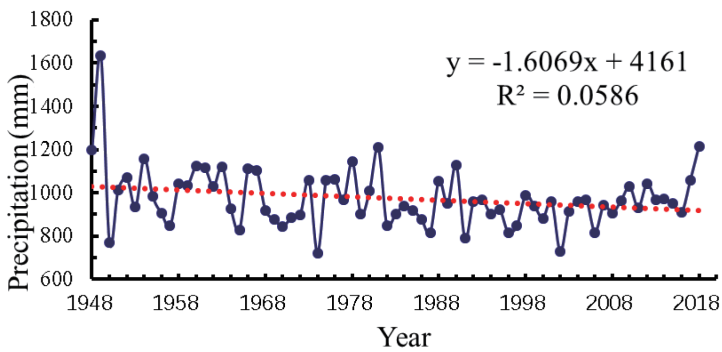

Fig. 6. (Color online) Annual precipitation in Longxi River Basin from 1948 to 2018.

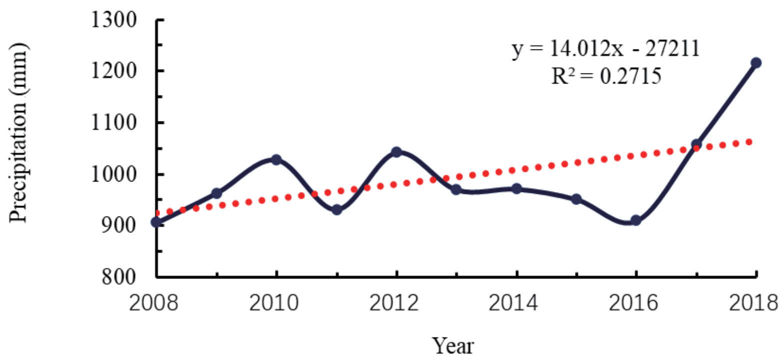

Fig. 7. (Color online) Annual precipitation in Longxi River Basin from 2008 to 2018.

4.3 Seasonal variation of precipitation

In this region, there is a large difference in precipitation among the four seasons, so the variation of precipitation in the different seasons is analyzed. Figures 8–11 depict the variation of average precipitation from 1948 to 2018 in spring (March to May), summer (June to August), fall (September to November), and winter (December to February), respectively.

The trend equation and R^2 in spring from 1948 to 2018 are as follows:

$$y = 0.0641x - 62.749,\ R^2 = 0.0149 \text{ (1948 to 2018)}. \tag{5}$$

From Fig. 9, we can see that the precipitation in summer shows a downward trend, with obvious fluctuations. Higher precipitation can be observed in summer than in the other seasons.

The trend equation and R^2 in summer from 1948 to 2018 are as follows:

$$y = -0.3739x + 914.97,\ R^2 = 0.0446 \text{ (1948 to 2018)}. \tag{6}$$

Figure 10 shows that the change in precipitation in fall after the earthquake is gentler than that before the earthquake.

The trend equation and R^2 in fall from 1948 to 2018 are as follows:

$$y = -0.2374x + 547.69,\ R^2 = 0.06 \text{ (1948 to 2018)}. \tag{7}$$

Finally, from Fig. 11 we can see that the precipitation in winter is less than that in the other seasons. The variation of precipitation from year to year in winter is larger than that in the other seasons, and the long-term trend of the precipitation shows a slight increase.

The trend equation and R^2 in winter from 1948 to 2018 are as follows:

$$y = 0.0176x - 25.027,\ R^2 = 0.01 \text{ (1948 to 2018)}. \tag{8}$$

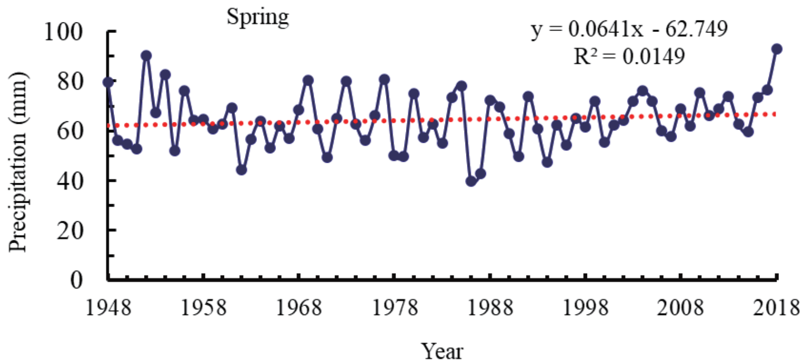

Fig. 8. (Color online) Precipitation in Longxi River Basin during spring from 1948 to 2018.

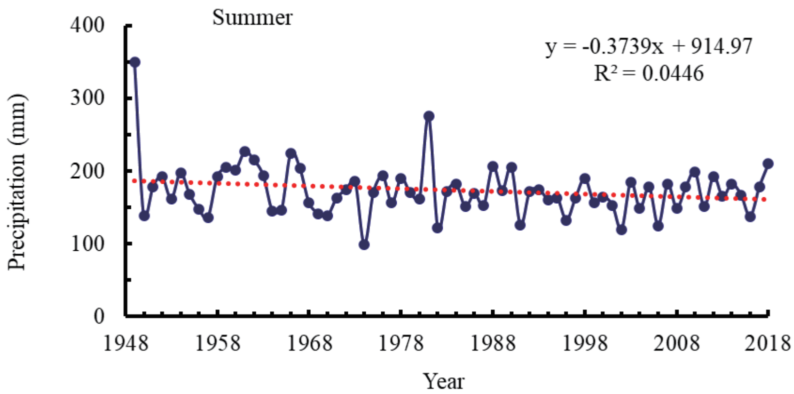

Fig. 9. (Color online) Precipitation in Longxi River Basin during summer from 1948 to 2018.

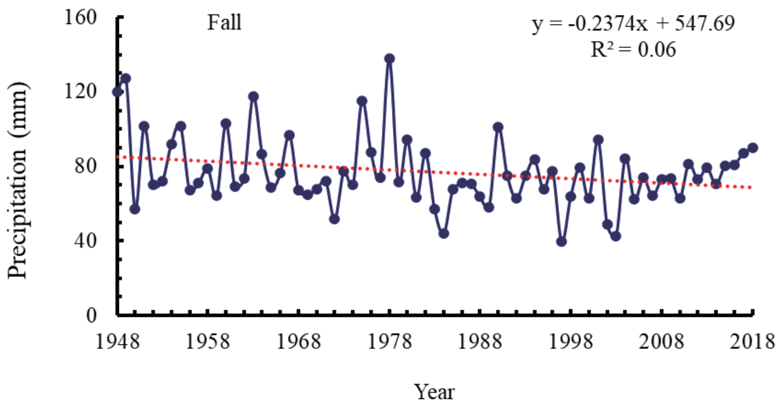

Fig. 10. (Color online) Precipitation in Longxi River Basin during fall from 1948 to 2018.

Vegetation cover has a great impact on the moisture content and convective activity in the atmosphere. The total amount of water vapor entering the atmosphere increases significantly with vegetation cover. The convective activity at large and small scales is strengthened, regional precipitation is increased, and the number of days without precipitation is reduced. Surfaces without vegetation cover show the opposite behavior.[31]

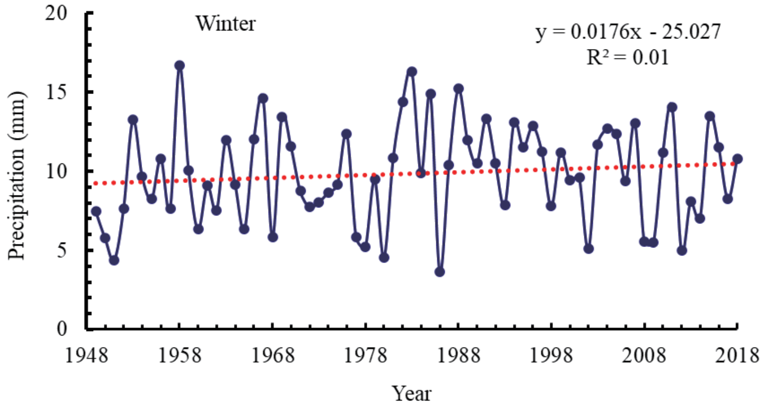

Fig. 11. (Color online) Precipitation in Longxi River Basin during winter from 1948 to 2018.

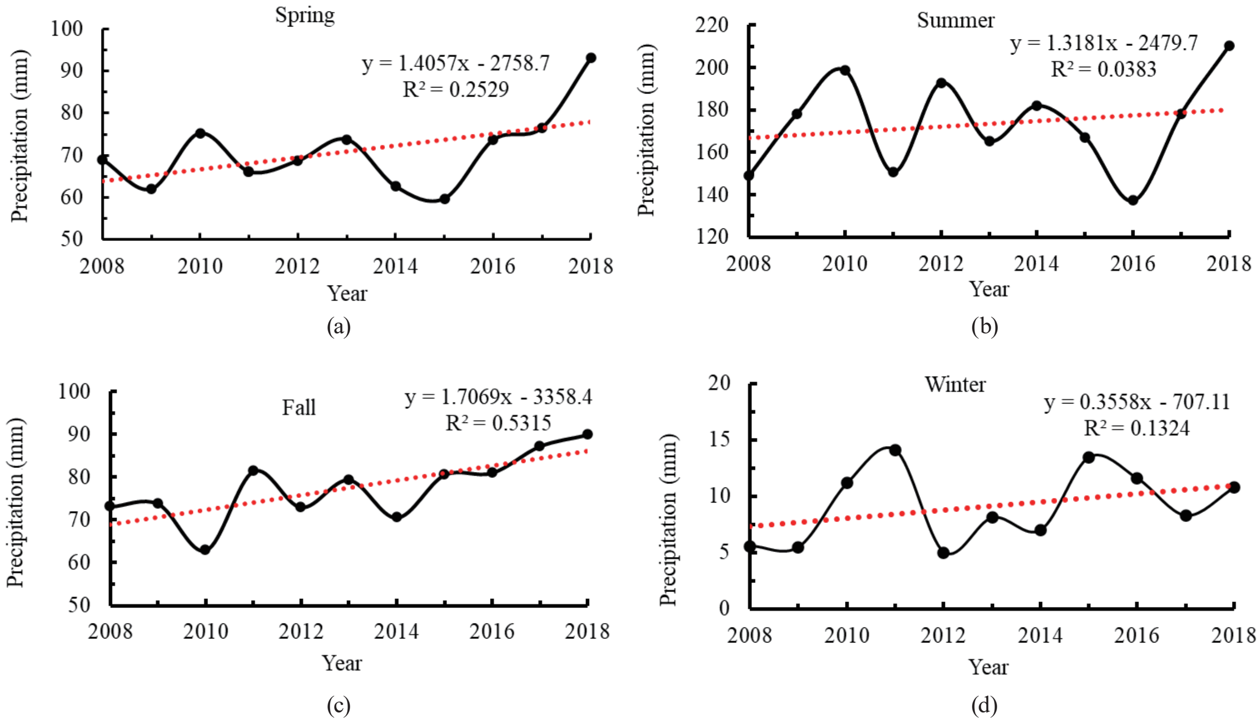

Fig. 12. (Color online) Precipitation in Longxi River Basin in different seasons from 2008 to 2018.

Figures 12(a)–12(d) show the precipitation in the Longxi River Basin in spring, summer, fall, and winter from 2008 to 2018, respectively. From the figure, the precipitation in the four seasons fluctuates greatly, but the overall trend is a significant increase.

From the above, it can be seen that with the recovery of vegetation (i.e., increase in NDVI) after the earthquake in 2008, the annual precipitation increased by 14.012 mm and the precipitation of the different seasons also showed an increasing trend between 2008 and 2018, indicating that vegetation has some effect on the regional precipitation. Thus, an increase in precipitation clearly indicates an increase in vegetation and vice versa. The regression trend equations and R^2 of precipitation in the different seasons from 2008 to 2018 are as follows:

$$y = 1.4057x - 2758.7, R^2 = 0.2529 \text{ in spring (2008 to 2018)}, \quad (9)$$

$$y = 1.3181x - 2479.7, R^2 = 0.0383 \text{ in summer (2008 to 2018)}, \quad (10)$$

$$y = 1.7069x - 3358.4, R^2 = 0.5315 \text{ in fall (2008 to 2018)}, \quad (11)$$

$$y = 0.3558x - 707.11, R^2 = 0.1324 \text{ in winter (2008 to 2018)}. \quad (12)$$

5. Discussion

5.1 Effect of vegetation on surface reflectance[32–36]

Vegetation is the principal part of the terrestrial ecosystem and can conserve water and regulate temperature and humidity. One of its important functions is to produce rain (snow)-forming clouds. The process of large-scale cloud formation on land is the result of atmospheric circulation. In addition to its role in atmospheric circulation, the vegetation on the earth's surface also has a certain impact on the precipitation process in some areas. Vegetation is the main factor affecting surface reflectance. Vegetation can change the reflectivity of the earth's surface and provide biological nuclei for raindrops. Although the earth receives solar short-wave radiation, it continuously radiates long-wave radiation. The atmosphere around the earth absorbs relatively little solar short-wave radiation, but the ground strongly absorbs long-wave radiation. In addition, the atmosphere itself emits long-wave radiation. Therefore, during the exchange of heat between the atmosphere and the ground, some heat is also dissipated to space. The heat on the earth's surface is mainly received from solar radiation. However, the surface also reflects part of the heat. The ability to reflect heat, i.e., surface reflectance, depends on the surface conditions. The surface state refers to the surface color, humidity, temperature, and roughness. Dark ground absorbs most of the solar radiation, whereas light ground reflects most of the solar radiation. The color of the ground surface is related to the amount of vegetation, where vegetation is darker than bare land. Humus soil containing plant debris is darker and gray-black; native soil lacking plant debris is lighter and yellow-brown; quicksand is white and light yellow. When the earth's surface is wet, its ability to absorb solar radiation is relatively high; when the surface is dry, its ability to reflect light radiation is relatively high. This is because the evaporation of surface water consumes a large amount of solar energy. The water storage capacity of vegetation is relatively high, and there is a lot of water under vegetation. Therefore, the ability of vegetation to absorb solar radiation is relatively high. Bare land without vegetation is dry and strongly reflects solar radiation. The surface temperature also affects the reflectivity, with the reflectivity increasing proportionally with the surface temperature. Where there is vegetation, the surface temperature is lower, and so is the reflectance; on bare surfaces without vegetation (such as the Gobi desert), the surface temperature and reflectance are both high. Finally, the lower the roughness (unevenness) of the earth's surface, the greater the reflectivity. Bare land (such as the

Gobi desert) has low roughness, grassland and forest have higher roughness, and regions where forest, trees, shrubs, and artemisia grass coexist have high roughness.

In the "5.12" Wenchuan earthquake disaster area, secondary disasters after the earthquake included collapses, landslides, debris flows, and unstable slopes, which resulted in the accumulation of a large amount of materials deposited on slopes or gullies. This led to large areas of exposed rocks, reducing surface vegetation coverage and roughness and increasing reflectance.

5.2 Surface reflectivity and precipitation

The underlying cause of land-based cloud precipitation is atmospheric circulation. Water vapor from the oceans moves inland to the continent and produces rain. In the presence of water vapor, the development of precipitation-forming clouds in local areas on the land is largely determined by the condition of the surface vegetation. Where there is luxuriant vegetation, the probability of precipitation will be higher. The effect of surface vegetation on regional precipitation is mainly through changes in surface roughness and surface albedo, which affect the energy exchange between the earth and the atmosphere, changing the heat and momentum budgets and the convection between the earth and the atmosphere, thus causing regional changes in climate.[37]

Atmospheric precipitation is the result of repeated water circulation. Water vapor forms clouds, resulting in rain. The reflectivity of the earth's surface directly affects precipitation. For a surface with low reflectivity, owing to the absorption of more solar radiation, the surface temperature increases, and the evaporation of water vapor is higher, which is conducive to the propagation and rise of marine water vapor. The vapor cools and condenses in the troposphere to form clouds, then precipitation occurs. This is related to the high probability of precipitation in places with a lot of vegetation. In places with high reflectance, owing to the large loss of solar radiant heat, the surface temperature drops, forming dry and cold air in the troposphere, which curbs the rise of heated air, thus preventing the conditions required for precipitation to occur. Since the heated air contains a large amount of water vapor, without the rise of the warm and wet air flow, there will be no precipitation. The reflectivity of the earth's surface directly affects the rise of warm and wet air and the fall of dry and cold air, which result in precipitation and the suppression of rain, respectively. Vegetation affects cloud formation by evapotranspiration, leading to precipitation, which leads to a change in local microclimate.

After the Wenchuan earthquake, because of the increased surface reflectance due to the large area of exposed rocks, precipitation was inhibited compared with that before the earthquake. With the gradual recovery of vegetation and the increase in surface roughness, the reflectivity gradually decreased and the level of precipitation returned to that before the earthquake.

5.3 Relationship between vegetation and local precipitation

The variation of precipitation is mainly affected by the topography, climate (wind zone, pressure, and monsoon), ground water, and so forth. Interannual changes in vegetation coverage are mainly attributed to climate fluctuation and human activities. Precipitation is the most important factor limiting the growth of natural vegetation.(38) Therefore, in the short term, the amount of precipitation and its distribution are the most significant factors affecting vegetation cover during a year. The variation of vegetation also affects the local climate. The mechanism by which vegetative cover affects the climate is complex and differs in different regions.

The growth of vegetation affects the regional climate through the exchange of water, momentum, and energy between land and air, as well as through various processes, such as gas emission.(39) In addition to the regional scale, vegetation can also affect large-scale circulations by affecting local atmospheric circulation or bio-geochemical cycles, ultimately causing large-scale climate changes and even changes in global climate. In recent years, remote sensing technology has been used to simulate and diagnose the interaction between vegetation coverage and climate change.(40–44) Previous studies have shown that vegetation has a significant impact on the surface temperature and precipitation in China. NDVI is positively correlated with precipitation in most parts of China, although there are regional differences in correlation between these two factors.(45)

Studies on the relationship between vegetation changes and precipitation have found that they can affect each other. Generally, local vegetation is less affected by precipitation in the case of sufficient precipitation or satisfactory irrigation conditions.(15) Some scholars believe that forests can enhance precipitation to a certain extent, and the effect of changes in vegetation on precipitation increases with decreasing atmospheric humidity. Some studies have suggested that vegetation has little effect on precipitation.

6. Conclusion

In this study, Terra MODIS sensor NDVI daily data with 500 m resolution and remote sensing images were used to analyze the effect of vegetation changes on precipitation in the Longxi River Basin after the Wenchuan earthquake. Surface vegetation changed after the Wenchuan earthquake (NDVI values were 0.394 in 2007 and 0.383 in 2008) and surface characteristics changed accordingly (such as surface albedo, surface roughness, and soil moisture). The changes in surface characteristics affected the radiant flux and effective heat flux (sensible heat flux and latent heat flux) in the study area. With the decrease in vegetation cover, surface roughness, the water holding capacity of soil, soil water content, and surface evapotranspiration decreased owing to the increase in latent heat flux. These changes affected the precipitation in the study area [the annual precipitation in 2008 was 905.3 mm, which was the lowest during the period of observation (2008–2018), and the highest annual precipitation occurred in 2018 (1215.6 mm)].

It was found that vegetation coverage decreased owing to secondary geological disasters after the earthquake, resulting in decreased mean values of vegetation coverage. From 1948 to 2018, the annual and seasonal (except in winter) precipitation in the basin decreased. With the artificial and natural recovery of vegetation after the earthquake, vegetation coverage increased, annual precipitation increased, and the precipitation in different seasons exhibited an increasing trend.

The mechanism by which vegetation affects climate differs in different regions. Scientifically exploring the impact of vegetation on climate in different regions is conducive to the formulation of climate and ecological environmental protection and improvement programs. The cause of precipitation on land is atmospheric circulation. In the presence of water vapor, the development of rain-forming clouds in local areas is mainly determined by the condition of surface vegetation in the Longxi River Basin: where there is more (less) vegetation, the probability of precipitation is higher (lower). Vegetation affects the development of rain-forming clouds and can change local microclimates. The increasing frequency of droughts has seriously threatened people's lives and sustainable economic development. Since vegetation has an effect on cloud precipitation, natural vegetation should be protected in arid and rain-stricken areas, and more artificial forests should be created to increase precipitation.

Author Contributions

Conceptualization, Biyun Guo; Methodology, Biyun Guo, Mantravadi Venkata Subrahmanyam; Software, Mantravadi Venkata Subrahmanyam; Investigation, Aiguo Li, Guangzhe Liu; Original Draft Preparation, Biyun Guo; Reviewing & Editing, Biyun Guo, Mantravadi Venkata Subrahmanyam; Project Administration, Biyun Guo; Funding Acquisition, Biyun Guo. All authors have read and agreed to the published version of the manuscript.

Acknowledgments

This study was supported by the State Key Laboratory of Plateau Ecology and Agriculture, Qinghai University (Grant No. 2018-KF-02), the open research fund program of State Key Laboratory of Hydroscience and Engineering, Tsinghua University (SKLHSE-2021-B-01), the National Natural Science Foundation of China (Grant Nos. 51479179 and 51579230), the Science Foundation of Zhejiang Ocean University (Grant No. 21105011713), and Innovation and Development of Social Science in Anhui Province (No. 2019CX016).

Conflict of Interest

The authors declare no competing interests.

References

1 W. Wang, Y. Pan, W. Xu, J. Wang, and X. Bai: Res. Environ. Sci. **21** (2008) 110 (in Chinese).
2 P. Cui, Y. Lin, and C. Chen: Ecol. Eng. **44** (2012) 61. https://doi.org/10.1016/j.ecoleng.2012.03.012
3 Z. Li, Q. Jiao, L. Liu, H. Tang, and T. Liu: ISPRS Int. J. Geo-Inf. **3** (2014) 368. https://doi.org/10.3390/ijgi3010368
4 P. Cui, Y. Zhu, Y. Han, X. Chen, and J. Zhuang: Landslides **6** (2009) 209. https://doi.org/10.1007/s10346-009-0160-9
5 J. Han, S. Wu, S. He, W. Sun, C. Zhang, and T. Wang: Earth Sci. Fontiers **16** (2009) 306 (in Chinese). https://doi.org/10.1097/00054725-200912002-00062
6 H. Xing and X. Xu: M8.0 Wenchuan Earthquake (Springer-Verlag, Berlin, Germany, 2011).
7 M. Zhu, L. Shen, Vivian W. Y. Tam, Z. Liu, T. Shu, and W. Luo: Sci. Total Environ. **714** (2020) 136843. https://doi.org/10.1016/j.scitotenv.2020.136843
8 C. A. Nobre, P. J. Sellers, and J. Shukla: J. Climate **4** (1991) 957. https://doi.org/10.1175/1520-0442(1991)004<0957:ADARCC>2.0.CO;2
9 J. E. Bagley, A. Desai, K. J. Harding, and P. K. Snyder: J. Climate **27** (2014) 345. https://doi.org/10.1175/JCLI-D-12-00369.1

10 Y. Xue, K. Liou, and A. Kasahara: J. Climate **3** (1990) 337. https://doi.org/10.1175/1520-0442(1990)003<0337:IOBFOT>2.0.CO;2
11 S. Wang: Aridity Trend in Northern China (Springer, Berlin, Heidelberg, Germany, 2017)
12 F. Dai, C. Xu, X. Yao, L. Xu, X. Tu, and Q. Gong: J. Asian Earth Sci. **40** (2011) 883. https://doi.org/10.1016/j.jseaes.2010.04.010
13 S. Qi, Q. Xu, and H. Lan: Eng. Geol. **116** (2010) 95. https://doi.org/10.1016/j.enggeo.2010.07.011
14 C. Xu, X. Xu, X. Yao, and F. Dai: Landslides **11** (2013) 441. https://doi.org/10.1007/s10346-013-0404-6
15 S. Zhang, L. Zhang, and T. Glade: Eng. Geol. **175** (2014) 175. http://dx.doi.org/10.1016/j.enggeo.2014.03.012
16 Z. Wu, P. J. Barosh, Z. Zhang, and H. Liao: Eng. Geol. **28** (2012) 143. https://doi.org/10.1016/j.enggeo.2012.06.006
17 G. Liu, J. Li, and Z. Xu: Int. J. Appl. Earth Obs. **12** (2010) 496. https://doi.org/10.1016/j.jag.2010.05.005
18 F. Chen, H. Guo, N. Ishwaran, W. Zhou, R. Yang, L. Jing, F. Chen, and H. Zeng: Remote Sens. **6** (2014) 6283. https://doi.org/10.3390/rs6076283
19 C. Fu and H. Yuan: Chin. Sci. Bull. **46** (2001) 691 (in Chinese).
20 Z. Xiong: Simulation and Analysis of Eastern Asian Climate and Its Inter Annual Variability by Regional Climate Model, Doctoral Thesis (Institute of Atmospheric Science, Chinese Academy of Science, Beijing, 2001) (in Chinese).
21 D. V. Spracklen and L. Garcia-Carreras: Geophys. Res. Lett. **42** (2015) 9546. https://doi.org/10.1002/2015GL066063
22 Z. Wang, P. Cui, and H. Liu: J. Hydraul. Eng. **41** (2010) 757 (in Chinese).
23 J. S. Becker, D. M. Johnston, D. Paton, G. T. Hancox, T. R. Davies, M. J. Mcsaveney, and V. R. Manville: Nat. Hazards Rev. **8** (2007) 35. https://doi.org/10.1061/(ASCE)1527-6988(2007)8:2(35)
24 P. Cui, K. Hu, J. Zhuang, Y. Yang, and J. Zhang: J. Mt. Sci. **8** (2011) 1. https://doi.org/10.1007/s11629-011-2040-8
25 C. Tang, J. Zhu, W. Li, and J. Liang: B. Eng. Geol. Environ. **68** (2009) 187. https://doi.org/10.1007/s10064-009-0201-6
26 L. Garrote and R. L. Bras: J. Hydrol. **167** (1995) 279. https://doi.org/10.1016/0022-1694(94)02592-Y
27 P. Cui, Y. Lin, and C. Chen: Ecol. Eng. **44** (2012) 61. https://doi.org/10.1016/j.ecoleng.2012.03.012
28 P. Cui: Environ. Earth Sci. **65** (2012) 963. https://doi.org/10.1007/s12665-012-1521-6
29 G. J. Huffman, R.F. Adler, M. Morrissey, D .T. Bolvin, S. Curtis, R. Joyce, B. McGavock, and J. Susskind: J. Hydrometeorol. **2** (2001) 36. https://doi.org/10.1175/1525-7541(2001)002<0036:GPAODD>2.0.CO;2
30 GPCP Version 1.3 Data: https://climatedataguide.ucar.edu/climate-data/gpcp-monthly-global-precipitation-climatology-project (access December 2018).
31 W. Ma, Z. Zhao, X. Liu, and D. Yan: Remote Sens. Land Resour. **87** (2010) 109 (in Chinese).
32 A. W. R. Seddon, M. Macias-Fauria, P. R. Long, D. Benz, and K. J. Willis: Nature **531** (2016) 229. https://doi.org/10.1038/nature16986
33 Y. Wang and Y. Luo: Sci. Total Environ. **693** (2019) 133553. https://doi.org/10.1016/j.scitotenv.2019.07.359
34 Z. Zhang, J. Liu, and X. Gu: Land Use Policy **82** (2019) 620. https://doi.org/10.1016/j.landusepol.2018.12.040
35 J. Du, Z. He, J. Yang, L. Chen, and X. Zhu: Int. J. Remote Sens. **35** (2004) 6490. https://doi.org/10.1080/01431161.2014.955146
36 Z. He, J. Du, W. Zhao, J. Yang, L. Chen, X. Zhu, X. Chang, and H. Liu: Agric. For. Meteorol. **213** (2015) 42. https://doi.org/10.1016/j.agrformet.2015.06.013
37 G. Fan and S. Li: Plateau Meteorol. **18** (1999) 649 (in Chinese).
38 Y. Wu, A. Huang, D. Huang, F. Chen, B. Yang, Y. Zhou, D. Fang, L. Zhang, and L. Wen: Clim. Dynam. **51** (2018) 4287. https://doi.org/10.1007/s00382-017-4042-x
39 D. Halwatura and M. M. M. Najim: Environ. Modell. Softw. **46** (2013) 155. http://doi.org/10.1016/j.envsoft.2013.03.006
40 P. B. Hunukumbura, S. B. Weerakoon, and S. Herath: Traversing No Man's Land, Interdisciplinary Essays in Honor of Professor Madduma Bandara, N. Hennayake, N. Rekha, M. Nawfhal, R. Alagan, and C. Daskon, Eds. (University of Peradeniya, Peradeniya, Sri Lanka, 2008) pp. 169–184.
41 T. Deng: Study the Development Regularity and Control Measures in Longchi before and after the "5.12" Earthquake, Master's Thesis (Chengdu University of Technology, Cheng Du, China, 2011) (in Chinese).
42 B. Yu, Y. Ma, and J. Zhang: J. Mountain Science **29** (2011) 738 (in Chinese). http://doi.org/10.1007/s12583-011-0163-z
43 P. Cui, S. He, and L. Yao: Formation Mechanism and Risk Control in Wenchuan Earthquake of Mountain Disaster (Science Press, Beijing, China, 2011) (in Chinese).
44 S. Chu, B. Yu, and L. Li: Soil Water Conserv. Chin. **11** (2011) 52 (in Chinese). http://doi.org/10.14123/j.cnki.swcc.2011.08.001
45 J. Zhang, W. Dong, C. Fu, and L. Wu: Adv. Atmos. Sci. **20** (2003) 1002. http://doi.org/10.1007/bf02915523